

# Immunocytochemical and Electrophoretic Distribution of Cytokeratins in the Resting Stage Epidermis of the Lizard *Podarcis sicula*

LORENZO ALIBARDI,\* MARIAGABRIELLA MAURIZII, AND CARLO TADDEI

*Dipartimento di Biologia Evoluzionistica Sperimentale, University of Bologna, 40126 Bologna, Italy*

**ABSTRACT** The distribution of three anti-cytokeratin ( $\alpha$ -keratin) antibodies (AE1, AE2, AE3) in the epidermis of a lizard has been studied by immunocytochemistry at light and electron microscope and by immunoblot analysis. This study shows the expression of different keratins in the resting stage epidermis of the lizard *Podarcis sicula*. In this stage the epidermis has an external  $\beta$ -layer, an underlying  $\alpha$ -layer, some layers of living suprabasal cells and a basal stratum germinativum. The AE1 antibody is localized in the basal and suprabasal cells only in the outer scale surface, but is absent from the inner surface, the hinge region and from the keratinized  $\beta$ - and  $\alpha$ -layers. The AE2 antibody is mainly localized at the level of the hinge region and of the  $\alpha$ -layer and gives a lower reaction in the  $\beta$ -layer. The AE3 antibody is mainly localized in basal and suprabasal cells, lower in the  $\alpha$ -layer, and absent from the  $\beta$ -layer. The electron microscope shows that all the three antibodies immunolabel cytoplasmic fibrillar structures in the deep  $\alpha$ -layers and that AE2 and AE3 antibodies label small electron-dense areas in the external dense  $\beta$ -layer within the electron-lucid matrix. Immunoblot analysis of the keratins extracted and separated by gel electrophoresis demonstrates the presence of a band of high molecular weight (67–68 kDa) positive to all three antibodies. In addition AE1 antibody recognizes a 44–45 kDa band and a 57–58 kDa band, AE2 recognizes a 60–61 kDa band, and AE3 recognizes a 47 kDa and a 56–57 kDa band. The localization of the keratins identified by immunoblot analysis in the epithelial layers is discussed taking in account the immunolabeling at light and electron microscope. The present study suggests that also in the normal epidermis of this reptiles, in both the  $\alpha$ - and the  $\beta$ -layer, the molecular masses of keratins increase from the basal to the keratinized layers, a phenomenon which is generalized to adult and embryonic amniotes epidermis. *J. Exp. Zool.* 289:409–418, 2001. © 2001 Wiley-Liss, Inc.

In mammalian epidermis cells are continuously produced in the basal layer, move upward, keratinize, and are desquamated (Matoltsy, '86; Fuchs, '90). During these processes, the composition of intermediate filaments varies and different cytokeratins ( $\alpha$ -keratins) are progressively produced, both in developing and adult epidermis (Moll et al., '82; Woodcock-Mitchell et al., '82; Sun et al., '83; Dale et al., '85, '87).

By contrast in lepidosaurian reptiles (most represented by lizards and snakes) epidermal cells are not produced continuously from the basal layer: the epidermis has resting phases alternated with renewal phases (Maderson et al., '72; Maderson, '85). This cyclical process is termed the shedding cycle. This unique, very complex, lepidosaurian phenomenon results in the formation of an outer epidermal generation, composed of six different keratinized layers (oberhautchen,  $\beta$ -, mesos,  $\alpha$ -,

lacunar, and clear), which is shed. Shedding reveals an incomplete epidermal generation (the previous inner unit) composed of only four layers (a new oberhautchen,  $\beta$ -, mesos, and an incomplete  $\alpha$ -layer) (Maderson et al., '98). Extensive morphological studies have characterized all the above epidermal layers in resting epidermis (Bryant et al., '67; Alexander, '70; Roth and Jones, '70; Maderson et al., '72; Landmann, '79, '86). Biochemical and X-ray diffraction studies have indicated that reptiles possess, like birds,  $\alpha$ - and  $\beta$ -keratins (Baden and Maderson, '70; Baden et al., '74; Wyld and Brush, '79, '83; Carver and

\*Correspondence to: Lorenzo Alibardi, Dipartimento di Biologia Ev. Sperm., University of Bologna, Via Selmi 3, 40126 Bologna, Italy.  
E-mail: alibardi@biblio.cib.unibo.it

Received 18 April 2000; Accepted 6 October 2000.

Sayer, '87). The  $\alpha$ - and  $\beta$ -keratins are different in molecular mass (MM), amino acid composition, and physico-chemical properties.

During a resting phase, little or no cell proliferation occurs, and this phase occupies most of the span of a shedding cycle. At specific periods, variable from species to species, epidermal cells of the basal layer resume proliferation and enter into a renewal phase. The latter lasts about 14 days in all the species of lepidosaurians so far studied, which is, incidentally, also the time that normally takes a mammalian keratinocytes to migrate from the basal layer to the keratinized layer (Dale et al., '87).

During the renewal phase three main processes take place: (1) the outer epidermal generation is completed with the addition of lacunar and clear layers, which fully mature; (2) beneath the outer generation another inner generation is formed, although incomplete; (3) at the end of the renewal phase the outer generation splits from the inner generation, and this determines the epidermal shedding (moult).

In reptiles, as in birds, the structural and functional differences between  $\alpha$ - and  $\beta$ -keratins are reported, and furthermore these two keratins are described as the products of a different set of genes (Carver and Sawyer, '87). In lepidosaurians the structure of the epithelial sheets suggest that these genes are probably activated and repressed in the vertical sequence of epidermal layers,  $\beta$ -keratins in oberhautchen and  $\beta$ -layer,  $\alpha$ -keratins in mesos,  $\alpha$ -layer, and lacunar and clear layers (Maderson, '85). The sequence of expression of  $\alpha$ -keratins in the epidermis of the first amniotes (the reptiles) is not known.

We have undertaken this study to clarify the keratins expressed in the basal epithelial layers of the lizard *Podarcis sicula* where the proliferation and early differentiation of the keratinocytes takes place. To localize and analyze the keratins expressed we have used three monoclonal antibodies (AE1, AE2, AE3), which in mammals recognize the most of the acidic and basic keratins (Sun et al., '83; Woodcock-Mitchell et al., '83; O'Guin et al., '87). Furthermore, this study was extended to the electrophoretic and immunoblotting analysis of the moults in order to identify the keratins present in the more external layers of the resting epidermis.

## MATERIALS AND METHODS

Adult lizards (*P. sicula*) of both sexes were used in this study. The animals were kept on a diet of

insects at room seasonal temperature in spring and summer. From five lizards, tissues were collected from the tail and belly and immersed in a modified Carnoy's Fixative (ethanol 95°/acetic acid 9:1) for 12–24 hr, dehydrated in ethanol, and embedded in wax. Using a rotatory microtome sections at 5–8  $\mu$ m were collected on polylysine-coated slides and stained for conventional light microscopy (1% toluidine blue) or for immunocytochemistry.

For immunocytochemistry the sections, pre-incubated for 45 min in sheep normal serum, were incubated overnight at 4°C with the primary antibody (mouse monoclonal AE1, AE2, AE3, from Progen, Heidelberg, Germany) at 1:130; 1:500; 1:130 in PBS (the primary antibody was omitted in the controls). Following repetitive rinsing in buffer, a secondary anti-mouse antibody conjugated to fluorescein (Silenus, Australia) was applied to the sections at a dilution of 1:20 in PBS. Sections were observed and photographed using a Zeiss microscope equipped with an epifluorescence-UV source using a fluorescein filter.

From five lizards, tissues were collected in 1–3-mm large pieces and fixed immediately in cold (0–4°C) 0.2% glutaraldehyde and 4% paraformaldehyde in 0.1 M phosphate buffer at pH 7.2–7.4 for 3–4 hr. Following buffer rinsing, the tissues were dehydrated and embedded in the acrylic resin (Bioacryl) at 4°C under UV illumination according to the method by Scala et al. ('92). After sectioning with an LKB NOVA ultramicrotome, thin sections were collected on nickel grids. The grids were incubated overnight at 4°C in the primary antibody (AE1, AE2 or AE3) at 1:40 dilution in Tris buffered saline (TBS) containing 0.1% Triton X and 1% cold water fish gelatin (CWFG) or 2% bovine serum albumin (BSA). After repeated rinses in TBS, the grids were incubated for 1 hr at room temperature with a goat anti-mouse IgG conjugated to 10-nm gold particles (Sigma) at a 1:40 dilution. The grids were rinsed in TBS and then in distilled water, and were then lightly stained in uranyl acetate–lead citrate for the observation with a CM 100 Philips electron microscope operating at 60–80 kV.

For the electrophoretic analysis, five lizards were decapitated; the skin was excised from the ventral and dorsal side of the body and cleaned of dermis. Numerous pieces of shed epidermis from different body areas were also collected for electrophoretic analysis. The cytokeratins were extracted from the epidermis as described by Achtstatter et al. ('86) and were separated in 10%

SDS-polyacrylamide gels according to Laemmli ('70). For immunoblotting, proteins were transferred to Hybond-C extra membranes (Amersham) as described by Towbin et al. ('79). The membranes were incubated with primary antibodies (AE1, 1:350; AE2, 1:500; AE3, 1:1,500), rinsed, incubated with the secondary antibody (alkaline phosphatase-conjugated, Sigma, 1:60,000), and the detection was done using 5-bromo-4-chloro-3-indolyl phosphate (BCIP, 0.66 mM) and with nitro blue tetrazolium (NBT, 0.32 mM; Promega).

## RESULTS

### *Epidermal histology and immunofluorescence*

The structure of the resting epidermis of *P. sicula* at the light microscope is shown in Fig. 1. At low magnification a cross-sectioned scale (Fig. 1A) has a dark and compact external  $\beta$ -layer lying above a darker  $\alpha$ -layer which, in longitudinal section (Fig. 1B), continues in the hinge region with those of the adjacent scale. At higher magnification (Fig. 1C,D) the basal and suprabasal cellular layers are easily identifiable. In Fig. 1D, which represents a longitudinal section of a scale, a flat suprabasal cell in the process of incorporation into the  $\alpha$ -layer is visible.

The structural organization of the resting epidermis is clarified in the schematic drawing (Fig. 1E) where the different epidermal layers are better evident (see figure legend for description).

Figure 2 reports the immunolocalization of the AE1, AE2, and AE3 antibodies in cross-sectioned scales where mostly the outer scale surface is present as shown in Fig. 1A. The AE1 antibody gives a clear labeling of basal and suprabasal living cells but abruptly decreases, or disappears, in the more external fully keratinized layers, especially in the outermost  $\beta$ -layer. Furthermore, the hinge regions between the scales remain completely unlabeled with this antibody (Fig. 2A,B). The AE2 antibody gives a clear fluorescence in the keratinized layers of the hinge region (Fig. 2C,E), in the  $\alpha$ -keratinized layer of the outer and inner scale surface, and a less intense fluorescence in the  $\beta$ -layer (Fig. 2C,D). This antibody does not react with epithelial cells of the basal and suprabasal layers which instead are heavily labeled with AE3 antibody (Fig. 2F,G). In the latter case the labeling, differently from that observed with AE1 antibody, continues in the hinge region of the scales. The fluorescent staining decreases in the  $\alpha$ -keratin layer and disappears in the  $\beta$ -layer (Fig. 2F,G).

### *Ultrastructural immunocytochemistry*

The immunoelectron localization of gold particles generally confirms the light microscopic study, although keratinized outermost layers appear more reactive in plastic sections than in paraffin sections. The AE1 antibody weakly labels keratin bundles in the basal and first suprabasal layer (Fig. 3A, inset at higher magnification), but it does not react in the keratinized layers (oberhautchen,  $\alpha$ -layers, and mesos). Only rare gold particles are present in more electron-dense spots scattered throughout the  $\beta$ -layer (Fig. 3A).

The AE2 labeling is almost absent in the oberhautchen and  $\beta$ -layer, with the exception of few darker areas among the electron-lucent  $\beta$ -keratin filaments (Fig. 3B). The labeling in the thin mesos cells beneath the  $\beta$ -layer is variable but generally less intense than that over the  $\alpha$ -cells present underneath (Fig. 3C,D). Instead the AE2 antibody gives a clear labeling with regularly distributed gold particles of the  $\alpha$ -layer (Fig. 3D). Bundles of suprabasal cells are labeled weakly or not at all with this antibody, while pre-keratinizing cells are sparsely labeled.

The AE3 antibody labels bundles of keratin filaments in all layers of the epidermis. Although they are not quantified, gold particles over the epidermal layers are more numerous than after the staining with AE2 or AE1 antibodies. The  $\beta$ -layer shows no labeling in the prevalent electron-lucent areas although there is an increase of diffuse labeling in the lowermost areas of the  $\beta$ -layer in contact the mesos layer (Fig. 3E,F). Specific labeling is, however, seen (more intense than using the AE2 antibody) over small electron-dense areas among the electron-lucent areas. The mesos layer shows a variable labeling, which increases in the underlying  $\alpha$ -layer (Fig. 3E). This antibody labels tonofilament bundles in basal and more intensely suprabasal cells. Furthermore immunogold particles are detectable in pre-keratinizing and keratinized  $\alpha$ -layers, including those over the hinge region (Fig. 3G,H). Also a diffuse immunolabeling, formed by clusters of gold particles, is seen over keratinized  $\alpha$ -cells.

### *Electrophoresis and immunoblotting*

The electrophoretic pattern of the whole epidermal extract after Coomassie blue staining shows several bands with a range of MM between 20 to over 100 kDa (Fig. 4A, lanes 1 and 2). The immunoblot analysis with AE1, AE2, and AE3 antibodies shows a clear band of 67–68 kDa positive to all three. With AE1, two weaker bands at

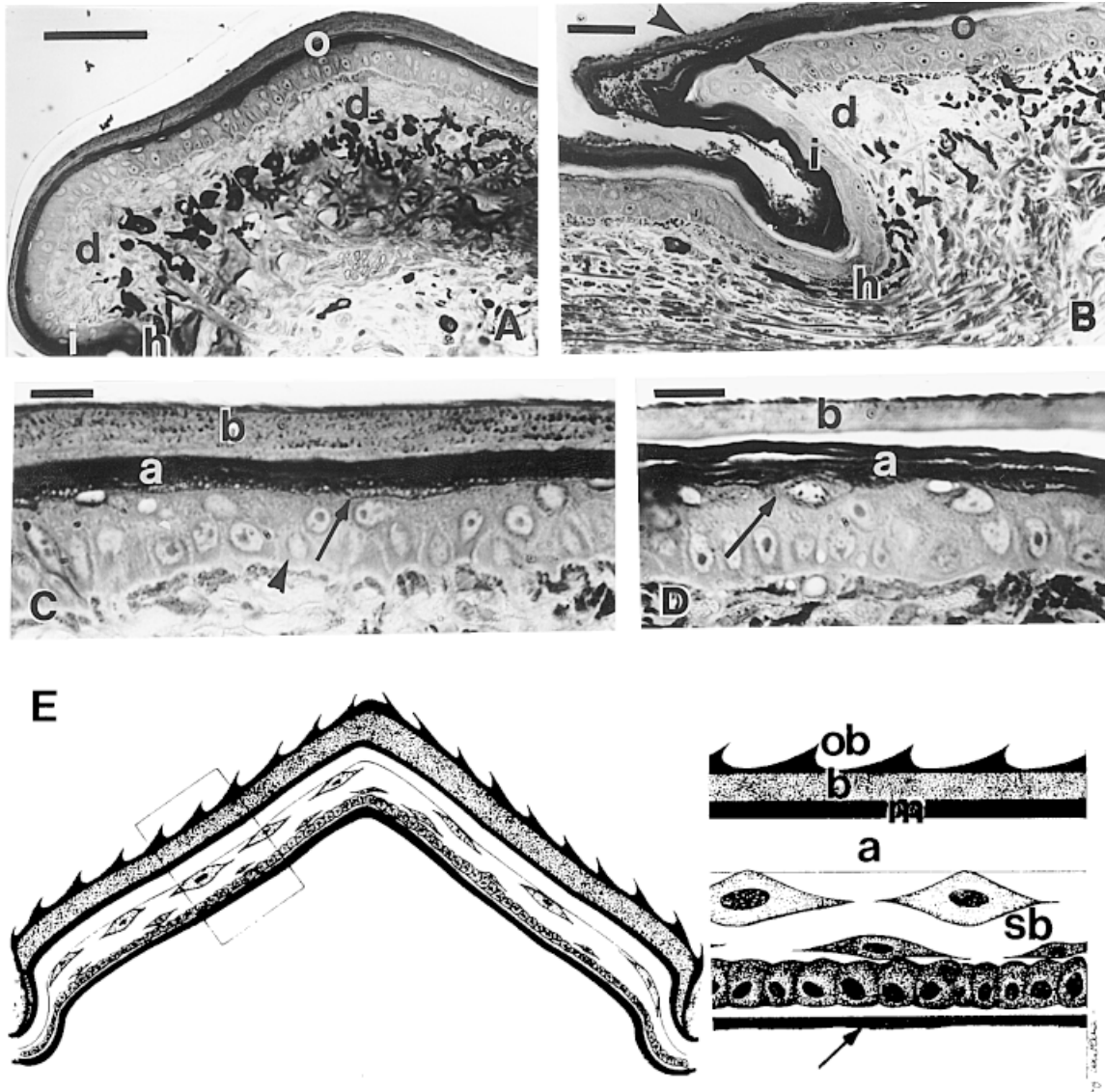


Fig. 1. **A:** Cross-section of resting tail scale featuring the outer (o) and inner (i) surfaces and hinge region (h). The dermis (d) is heavily pigmented. Scale bar, 50  $\mu$ m. **B:** Longitudinal section of tail scale showing the outer (o) and inner (i) surfaces, and the hinge region (h) under which the dermis (d) appears distorted. Arrowhead,  $\beta$ -layer; arrow,  $\alpha$ -layer. Scale bar, 25  $\mu$ m. **C:** Close-up of an area of outer scale surface featuring the paler  $\beta$ -layer (b), the darker  $\alpha$ -layer (a) with uncompact lowermost part (arrow) from the basal layer (ar-

rowhead). Scale bar, 10  $\mu$ m. **D:** Detail of epidermis of outer scale surface showing the  $\beta$ -layer (b) with the serrated outline of the external dark oberhautchen and the thick  $\alpha$ -layer (a) to which new cells are added (arrows). Scale bar, 10  $\mu$ m. **E:** Schematic drawing of a scale in cross-section during resting phase with all layers enlarged in the square. Ob, spinulated oberhautchen; b,  $\beta$ -layer; m, meso-layer; a,  $\alpha$ -layer; sb, suprabasal cells. The arrow points to the basement membrane beneath the basal layer.

57–58 kDa and 44–45 kDa, respectively, are detectable. With AE2, a strong band at 60–61 kDa becomes evident while AE3 shows two bands at 55–56 kDa and 47 kDa, respectively (Fig. 4A, lanes 3–5).

The electrophoretic pattern of the proteins of the shed epidermis (moult) is reported in Fig. 4B. A well-defined band of 67–68 kDa is evident,

and a more diffuse band within the range 60–64 kDa is visible underneath (Fig. 4B, lane 1). The immunoblot analysis of moult with the AE2 antibody shows two positive bands corresponding to 67–68 kDa and to 60–61 kDa respectively (Fig. 4B, lane 3), overlapping the pattern of normal (whole) epidermis (Fig. 4A, lane 4). The AE1 shows only a weak 67–68 kDa band which results

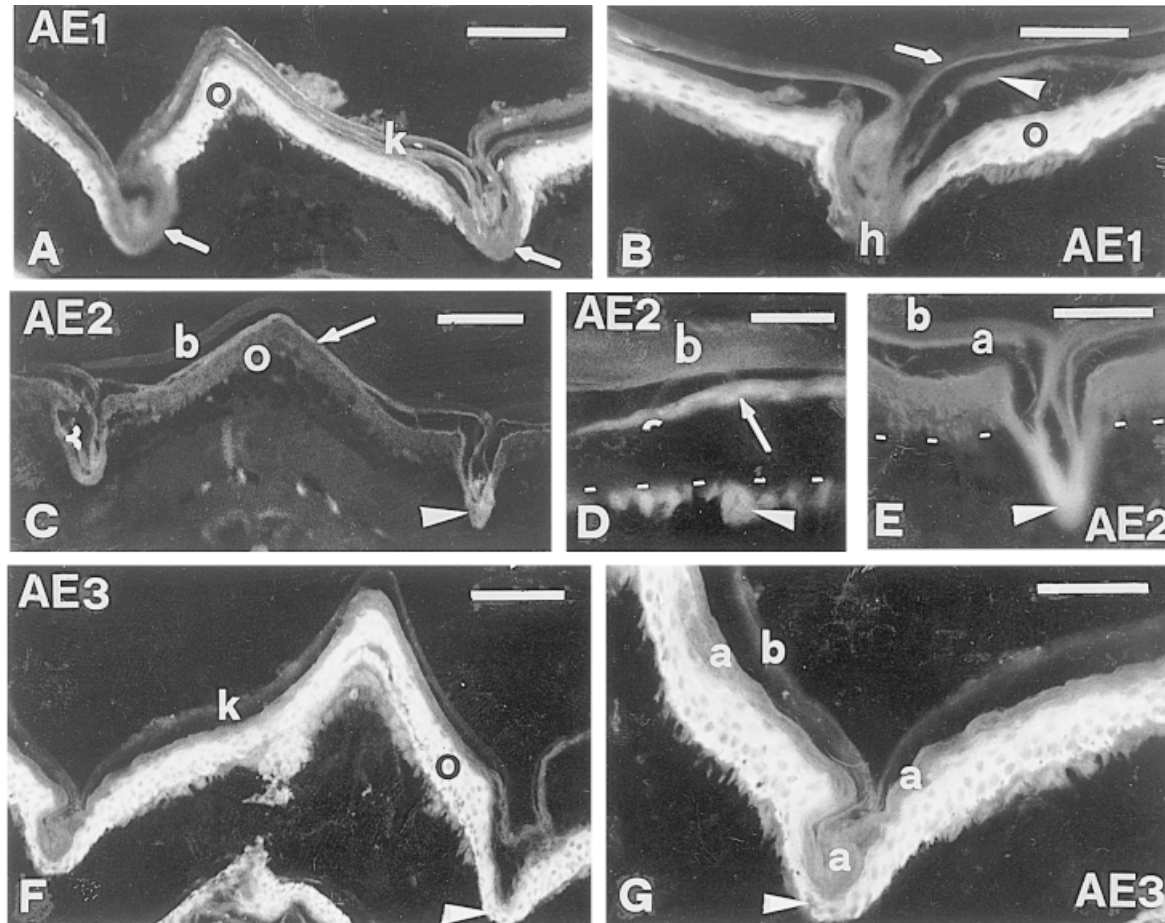


Fig. 2. **A,B:** AE1 antibody (AE1). **A:** the immunofluorescence is present in the living layers of the outer surface of the scale (o) beneath most immuno-negative keratinized layers (k) but is absent from the hinge regions (arrows). Scale bar, 100  $\mu$ m. **B:** close-up of the immuno-negative hinge region (h) which becomes intensely positive in the outer side (o) of the scale but almost disappears in the keratinized  $\alpha$ - (arrowhead) and  $\beta$ - (arrow) layers. Scale bar, 50  $\mu$ m. **C–E:** AE2 antibody (AE2). **C:** Fluorescence is concentrated in the hinge region (arrowheads) and in lower amount in the thin  $\alpha$ -layer (arrow) and the  $\beta$ -layer (b) of the outer surface (o). Scale bar, 100  $\mu$ m. **D:** Detail of the outer scale surface showing a clearly positive  $\alpha$ -layer (arrow) and the  $\beta$ -layer (b). Dots underlie the basal layer. The arrowhead indicates

aspecific fluorescence of melanosomes. Scale bar, 25  $\mu$ m. **E:** Detail of hinge region showing the highest fluorescence in its keratinized layers (arrowhead), which continues into the  $\alpha$ -layer (a) of the outer scale surface. The  $\beta$ -layer (b) in this region is almost negative. Dots underlie the basal and suprabasal layers that show a pale background. Scale bar, 50  $\mu$ m. **F,G:** AE3 antibody (AE3). **F:** Immunofluorescence is diffuse over all the living layers of the outer (o) and inner scale surfaces, continues in the hinge region (arrowhead) but almost disappears from the keratinized layers (k). Scale bar, 100  $\mu$ m. **G:** Detail of hinge region (arrowhead) showing immunopositive basal cells, a decreased positivity in the  $\alpha$ -layer (a) and a very low fluorescence in the  $\beta$ -layer (b). Scale bar, 50  $\mu$ m.

more intense with AE3 antibody (Fig. 4B, lanes 2 and 4).

## DISCUSSION

### *General considerations*

The reported observations show that in the lizard *P. sicula*, as in mammals (Woodcock-Mitchell et al., '82; Sun et al., '83; Dale and Holbrook, '87; O'Guin et al., '87), different keratins are expressed in the differentiating epithelial layers.

The basal and supra-basal cell layers are immunolabeled with AE1 and AE3 antibodies but are negative to the AE2 antibodies. Furthermore, the cellular layers in correspondence with the hinge regions of the scales give a strong and clear fluorescence with AE3 antibody but are negative to the AE1 antibody, which reacts only with those cells on the outer scale surface. The immunoblot analysis with AE1 and AE3 antibodies shows a different pattern of the bands that can account

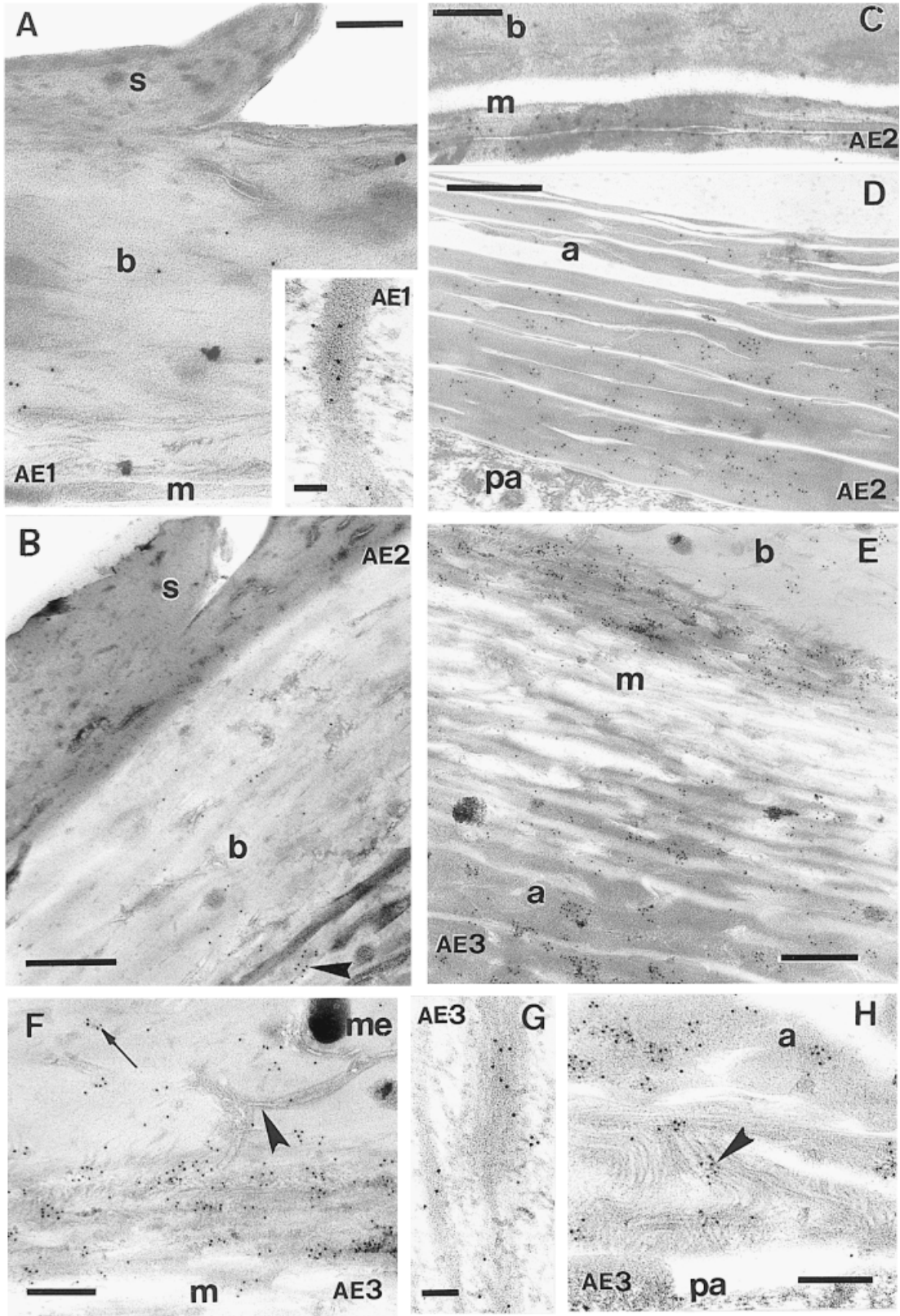


Fig. 3.

for the different immunolabeling of the two antibodies on the sections, in particular on the cell layers underneath the hinge region.

The keratinized  $\alpha$ - and  $\beta$ -layers give a poor reaction with all the antibodies with the exception of the AE2 antibody, which clearly labels the  $\alpha$ -layer. The low reactivity of these layers, in particular of the more compact  $\beta$ -layer, may be ascribed to technical and structural restrictions: the compact structure of the keratins may limit the reaction with the fluorochrome-labeled antibodies. In fact, at the electron microscope some gold particles are detectable in these layers. Furthermore the electrophoretic pattern and the immunoblotting of the shed epidermis (moult), which contains the two external layers, clearly shows the presence of two high MM keratin forms in these layers.

The immunoblot analysis of the epidermis with AE1, AE2, and AE3 antibodies shows three different patterns of keratins except for the 67–68 kDa band, which is recognized by all the antibodies used. Since this keratin form is also present in the moult preparations, its outermost localization in the epidermis is predictable. Furthermore, the reported observations show that the antigenicity of this keratin monomer, only detectable after biochemical separation, is somehow masked by the tissue treatments for light microscopy observations. The common immunoreactivity of this

high MM keratin to the antibodies here used can be explained as follows: (a) that the separated lizard cytoke­ratin monomer has some epitopes which are nonspecifically recognized by these antibodies produced in mammals or (b) that lizard keratins share epitopes recognized by these different monoclonal antibodies, like the common antigenic determinant shared by all classes of intermediate filaments (Pruss et al., '81).

Although we have not sectioned and made the immunoblot analysis of the single epidermal layers (an almost impossible task in the complex lizard epidermis), the present results suggests that a sequence of  $\alpha$ -keratins similar to that of the chick and mammals is also present in lizard epidermis (Fuchs and Marchuck, '83; Sawyer et al., '86; Bowden et al., '87; Carver and Sawyer, '88; Shames et al., '89; Fuchs, '90). The present study suggests that also in reptilian epidermis keratins with low molecular mass are produced in the lowermost layers (45, 50, and 58 kDa), their molecular mass increases in intermediate, prekeratinized, and keratinized  $\alpha$ - and  $\beta$ -layers (56–57 and 67–68 kDa), and that the keratins (60–61 kDa) in the stratum corneum are probably degradative products as suggested by Bowden et al. ('87) in mammals. Therefore, this sequence of keratins appears to be a generalized phenomenon in the epidermis of amniotes.

### *Cytokeratin localization in lizard epidermis*

In *Podarcis* the AE1-antibody stains not only basal cells (as in mammals) but also suprabasal cells, at least those of the outer surface of the scale, which will differentiate into  $\alpha$ - and  $\beta$ -cells. The hinge region, which is poorly or not stained by the AE1 antibody, lacks a  $\beta$ -layer and also a stratified  $\alpha$ -layer while only oberhautchen, mesos, lacunar, and clear cells have been described (Alexander, '70; Mittal and Singh, '87). The AE1 immunocytochemical pattern therefore appears to be linked to the degree of stratification but the immunofluorescence disappears in differentiating  $\alpha$ - or  $\beta$ -cells. While in mammals the AE1-antibody recognizes acidic cytoke­ratins with MW of 50 kDa and 57–58 kDa, in *Podarcis* it recognizes acidic cytoke­ratins with a relative low (44–45 kDa) or intermediate (57–58 kDa) MW. In mammals no AE1 antibody recognizes keratins with a MW above 58 kDa (Moll, '82; Sun et al., '83; O'Guin et al., '87). The fact the AE1 antibody recognizes a cytoke­ratin with a MW of 67–68 kDa suggests that in lizard this antibody recognizes a larger keratin than in mammals. The immunoblot

Fig. 3. Immunogold ultrastructural localization of AE1, AE2, and AE3 antibodies (AE1, AE2, AE3). **A:** With the AE1 antibody almost no labeling is seen in the spinulated fold (s) of the external oberhautchen fused to  $\beta$ -layer (b), and are also the thin cells of the mesos layer (m) negative. Scale bar, 200 nm. The inset shows labeling of a keratin bundle within a suprabasal cell. Scale bar, 100 nm. **B–D:** AE2 antibody. **B:** The spinulated folds of the oberhautchen (s) and  $\beta$ -layer (b) are almost negative. Arrowhead, labeled spot. Scale bar, 200 nm. **C:** Some gold particles are seen over the mesos cells (m) beneath the  $\beta$ -layer (b). Scale bar, 200 nm. **D:** Diffuse gold labeling of keratinized cells of the  $\alpha$ -layer (a) above a presumptive  $\alpha$ -cell (pa). Scale bar, 500 nm. **E–H:** AE3 antibody. **E:** Sparse gold particles are seen over the electron-pale  $\beta$ -layer (b) except for the region adjacent to the mesos layer (m). The immunolabeling increases in the  $\alpha$ -layer (a). Scale bar, 500 nm. **F:** Detail of the intensely immunolabeled lowermost region of the  $\beta$ -layer contacting the mesos cells (m). Gold particles specifically label some dark spots within the electron-lucent  $\beta$ -matrix (arrow). The arrowhead indicates cell membrane remnants of  $\beta$ -cells. Me, melanosome. Scale bar, 250 nm. **G:** Immunolabeled keratin bundle in suprabasal cell. Scale bar, 100 nm. **H:** Particular of passage region between pre- $\alpha$ -layer (pa) and fully  $\alpha$ -keratinized layer (a). The arrowheads points to labeled and still visible keratin filaments before their compacting in the mature  $\alpha$ -layer. Scale bar, 250 nm.

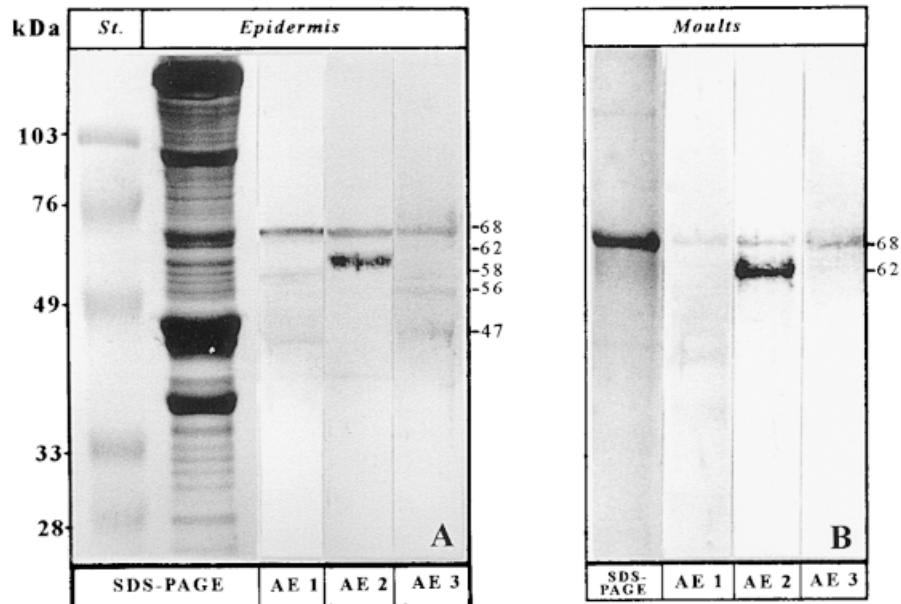


Fig. 4. **A:** Electrophoretic and immunoblotting patterns of whole epidermis. First left lane, MM standard (St). Second lane, Coomassie blue pattern. Third lane, AE1 immunostaining. Fourth lane, AE2 immunostaining. Fifth lane, AE3 immunostaining. **B:** Electrophoretic and immunoblotting pat-

terns of shed epidermal generation (moult). First lane, Coomassie blue pattern. Second lane, AE1 immunostaining. Third lane, AE2 immunostaining. Fourth lane, AE3 immunostaining.

analysis of moults, however, shows a very weak immunoreactivity for AE1 confirming the immunolocalization. The difference in immunoblots between whole epidermis and moults (containing only fully keratinized  $\alpha$ - and  $\beta$ -layers) indicates that mainly the 60–61 and 67–68 kDa keratins remains in these layers. Therefore, the keratins with lower MM are restricted in the living, pre-keratinized, layers. Because the 67–68 kDa cytokeratin is normally expressed in keratinized layers it is likely that the disappearance of AE1 immunoreactivity in suprabasal and keratinized layers takes place among the packing bundles of  $\alpha$ -keratin or among the packets of  $\beta$ -keratins. However, the low immunoreaction in moults suggests that this AE1 positive CK remains in small amount in the external keratinized layers. We suggest that the acidic cytokeratin with a MM of 57–58 kDa is localized in the suprabasal layer and the 44–45 kDa monomer (acidic) in the basal layer.

The AE2 antibody stains pre-keratinized and  $\alpha$ -keratinized layers but decreases and disappears in the  $\beta$ -layer. As in mammals, this antibody recognizes a 67–68 kDa band, but the main band has a 60–61 kDa MM. The latter monomer should therefore be responsible for the staining of the pre-keratinized and keratinized  $\alpha$ -layer in the outer and especially in the hinge region and be more

specific to stain keratin in cells destined to form the  $\alpha$ -layer, lacunar, and clear, that contain more  $\alpha$ -keratin at maturation than  $\beta$ -cells. This has been confirmed by the analysis of moults, which has identified only the two bands at 67–68 and 60–61 kDa (Fig. 4B). This pattern of distribution strictly resembles that of anti- $\alpha$ -keratin in scutate and scutellate scales of chicken (Sawyer et al., '86). Possibly, like in mammals (Bowden et al., '87), the 60–61 kDa cytokeratin (the AE2 specific band) can be a degradative product of the 67–68 kDa cytokeratin and contributes to the immunolabeling of the electron-dense areas within the  $\beta$ -layer.

The AE3 antibody stains the whole epidermis of *Podarcis* like that of mammals, although the  $\alpha$ -keratinized layer is less labeled than the living layers in paraffin-embedded epidermis while the  $\alpha$ -layer is the most labeled using immunogold on plastic sections. This may be due to different effects of the fixative and embedding procedure on the preservation or unmasking of antigenicity.

The decrease of immunofluorescence in the  $\beta$ -layer probably depends on the limited labeling in the small electron-dense areas within the tissue. During  $\beta$ -cell differentiation,  $\alpha$ -keratin filaments mix with  $\beta$ -keratin packets and are either partially diluted to a low level or are partially degraded by lysosomal enzymes (Landmann, '79;

Alibardi, '98c). Whatever the cause, some  $\alpha$ -keratin (basic) remains in the dense areas of the  $\beta$ -layer. The 60–61 kDa (AE2 positive) and the 55–56 kDa (AE3 positive) cytokeratins appear to be localized in these more electron-dense areas.

The specific bands at 55–56 kDa and 47 kDa (basic) are probably responsible for the epidermal staining of the suprabasal and basal layers, respectively (including those in the hinge region).

### *Reptilian and avian keratinization as compared to that of mammals*

The present study shows that all epidermal layers of a lizard, including those containing  $\beta$ -keratin (Oberhautchen and  $\beta$ -layer), contain  $\alpha$ -keratin, which has cross-reactive epitopes with those of mammals (O'Guin et al., '87). This confirms previous ultrastructural studies that showed  $\beta$ -keratin packets mixed with keratin bundles in adult resting (Roth and Jones, '68; Alexander, '70; Maderson et al., '72; Landmann, '79), embryonic (Alibardi, '98a,b; Alibardi and Thompson, '99), and regenerating epidermis (Alibardi, '95, '98c; Alibardi et al., 2000). The deposition of  $\beta$ -keratin in pre-formed bundles of  $\beta$ -keratin has also been observed in chick scutate scales (Carver and Sawyer, '88; Shames et al., '88, '89), feathers (Haake et al., '84; Meyer and Baumgartner, '98), beak (Shames et al., '91), and tongue (Carver and Sawyer, '89).

The deposition of  $\beta$ -keratin molecules on the scaffold of  $\alpha$ -filaments transforms the initially loose  $\alpha$ -keratin filaments into a compact and homogeneous mass where a 3–4 nm electron-lucent fibrils are seen (the  $\beta$ -keratin pattern, Alexander, '70; Baden and Maderson, '70; Baden et al., '74; Landmann, '79). In reptiles and birds (sauropsids) the deposition of  $\beta$ -keratin determines the hardening of external keratinocytes while  $\alpha$ -keratin is degraded or diluted within the  $\beta$ -keratin mass to such an extent that  $\alpha$ -keratin fibrils are no longer visible. The present immuno-electron microscopic study is the first to show that  $\alpha$ -keratin is still present within the mature  $\beta$ -layer of a reptile.

Differently from sauropsids, in mammals hard keratinized tissues such as hair and nails, keratin bundles are turned into compact masses but the diameter of electron-lucent keratin fibrils remains at 8–12 nm (the  $\alpha$ -pattern, Baden and Maderson, '70; Hashimoto, '71; Orwin, '79; Marshall et al., '91). The hardness of  $\alpha$ -keratinized tissues in mammals derives from the incorporation of high sulfur, high tyrosine, or high glycine matrix proteins among keratin filaments and not by another form of harder keratin (Marshall et al., '91).

### ACKNOWLEDGMENTS

This study was supported by a grant from Bologna University. Thanks to Mrs. Luciana Dipietrangelo for photographic work, to Ms. Federica Larotella (Disegno Anatomico, Bologna) for artwork, and to Prof. P.F.A. Maderson (Brooklyn College, CUNY, New York) for reading the manuscript. This work was supported by a 60% grant of the Bologna University and by a special research project "Segnali molecolari nello sviluppo" of the same University.

### LITERATURE CITED

- Achtstatter T, Hatzfeld M, Quinlan RA, Parmelee DC, Franke WW. 1986. Separation of cytokeratin polypeptides by gel electrophoretic and chromatographic techniques and their identification by immunoblotting. *Methods Enzymol* 134:355–371.
- Alexander NJ. 1970. Comparison of  $\alpha$  and  $\beta$  keratin in reptiles. *Z Zellforsch* 101:153–165.
- Alibardi L. 1995. Electron microscopic analysis of the regenerating scales in lizard. *Boll Zool* 62:109–120.
- Alibardi L. 1998a. Differentiation of the epidermis during scale formation in embryos of lizard. *J Anat* 192:173–186.
- Alibardi L. 1998b. Glycogen distribution in relation to epidermal cell differentiation during embryonic scale morphogenesis in the lizard *Anolis lineatopus*. *Acta Zool* 79:91–100.
- Alibardi L. 1998c. Presence of acid phosphatase in the epidermis of the regenerating tail of lizard (*Podarcis muralis*) and its possible role in the process of shedding and keratinization. *J Zool* 246:379–390.
- Alibardi L, Thompson MB. 1999. Epidermal differentiation during carapace and piastron formation in the embryonic turtle *Emydura macquarii*. *J Anat* 194:531–545.
- Alibardi L, Maurizii MG, Taddei C. 2000. Immunocytochemical and electrophoretic distribution of cytokeratins in the regenerating epidermis of the lizard *Podarcis muralis*. *J Morphol* 246:179–191.
- Baden HP, Maderson PFA. 1970. Morphological and biophysical identification of fibrous proteins in the amniote epidermis. *J Exp Zool* 174:225–232.
- Baden HP, Sviokla S, Roth I. 1974. The structural proteins of reptilian scales. *J Exp Zool* 187:287–294.
- Bowden PE, Stark HJ, Breikreutz D, Fusenig NE. 1987. Expression and modification of keratins during terminal differentiation of mammalian epidermis. In: Sawyer RH, editor. *Cell and molecular biology of keratins. Current topics in developmental biology*, Vol 22. Orlando, FL: Academic Press. p 35–68.
- Bryant SV, Breathnach AS, Bellairs d'AA. 1967. Ultrastructure of the epidermis of the lizard (*Lacerta vivipara*) at the resting stage of the sloughing cycle. *J Zool* 152:209–219.
- Carver WE, Sawyer RH. 1987. Development and keratinization of the epidermis in the common lizard, *Anolis carolinensis*. *J Exp Zool* 243:435–443.
- Carver WE, Sawyer RH. 1988. Avian scale development. XI. Immunoelectron microscopic localization of  $\alpha$  and  $\beta$  keratins in the scutate scale. *J Morphol* 195:31–43.
- Carver WE, Sawyer RH. 1989. Immunocytochemical localization and biochemical analysis of  $\alpha$  keratins in the avian lingual epithelium. *Am J Anat* 184:66–75.
- Dale AB, Holbrook KA, Kimball JR, Hoff M, Sun TT. 1985.

- Expression of epidermal keratins and filaggrin during human fetal skin development. *J Cell Biol* 101:1257–1269.
- Dale AB, Holbrook KA. 1987. Developmental expression of human epidermal keratins and filaggrin. In: Sawyer RH, editor. *Cell and molecular biology of keratins. Current topics in developmental biology*, Vol 22. Orlando, FL: Academic Press. p 127–151.
- Fuchs E. 1990. Epidermal differentiation: the bare essentials. *J Cell Biol* 111:2807–2814.
- Fuchs E, Marchuck D. 1983. Type I and type II keratins have evolved from lower eukaryotes to form the epidermal intermediate filaments in mammalian skin. *Proc Natl Acad Sci USA* 80:5857–5861.
- Haake AR, König G, Sawyer RH. 1984. Avian feather development: relationship between morphogenesis and keratinization. *Dev Biol* 106:406–413.
- Hashimoto K. 1971. Ultrastructure of human toenail. II. Keratinization and formation of the marginal band. *J Ultrastruct Res* 36:391–410.
- Laemmli UK. 1970. Cleavage of structural proteins during the assembly of the head of bacteriophage T4. *Nature* 227:165–176.
- Landmann L. 1979. Keratin formation and barrier mechanisms in the epidermis of *Natrix natrix* (Reptilia, Serpentes): an ultrastructural study. *J Morphol* 162:93–126.
- Landmann L. 1986. The skin of reptiles. Epidermis and dermis. In: Bereiter-Hahn J, Matoltsy AG, Sylvia-Richards K, editors. *Biology of the integument*, Vol 2, Vertebrates. Berlin: Springer-Verlag. p 150–187.
- Maderson PFA. 1985. Some developmental problems of the reptilian integument. In: Gans C, Billett F, Maderson PFA, editors. *Biology of the Reptilia*, Vol 14. New York: John Wiley & Sons. p 525–598.
- Maderson PFA, Flaxmann BA, Roth SI, Szabo G. 1972. Ultrastructural contribution to the identification of cell types in the lizard epidermal generation. *J Morphol* 136:191–210.
- Maderson PFA, Rabinowitz T, Tandler B, Alibardi L. 1998. Ultrastructural contributions to an understanding of the cellular mechanisms in lizard skin shedding with comments on the function and evolution of a unique lepidosaurian phenomenon. *J Morphol* 236:1–24.
- Marshall RC, Orwin DFG, Gillespie JM. 1991. Structure and biochemistry of mammalian hard keratin. *Electr Microsc Rev* 4:47–83.
- Matoltsy AG. 1986. The skin of mammals. Structure and function of the mammalian epidermis. In: Bereiter-Hahn J, Matoltsy AG, Sylvia-Richards K, editors. *Biology of the integument*, Vol 2, Vertebrates. Berlin: Springer-Verlag. p 255–271.
- Meyer W, Baumgartner G. 1998. Embryonal feather growth in the chicken. *J Anat* 193:611–616.
- Mittal AK, Singh JPN. 1987. Hinge epidermis of *Natrix piscator* during its sloughing cycle. Structural organization and protein histochemistry. *J Zool* 213:685–695.
- Moll R, Franke WW, Schiller DL, Geiger B, Krepler R. 1982. The catalog of human cytokeratins: patterns of expression in normal epithelia, tumors and cultured cells. *Cell* 31:11–24.
- O'Guin MW, Galvin S, Schermer A, Sun TT. 1987. Patterns of keratin expression define distinct pathways of epithelial development and differentiation. In: Sawyer RH, editor. *Cell and molecular biology of keratins. Current topics in developmental biology*, vol 22. Orlando, FL: Academic Press. p 97–125.
- Orwin DFG. 1979. The cytology and cytochemistry of the wool follicle. *Int Rev Cytol* 60:331–373.
- Pruss RM, Mirsky R, Raff MC, Thorpe R, Dowding A, Anderton BH. 1981. All classes of intermediate filaments share a common antigenic determinant defined by a monoclonal antibody. *Cell* 27:419–428.
- Roth SI, Jones WA. 1970. The ultrastructure of epidermal maturation in the skin of the boa constrictor (*Constrictor constrictor*). *J Ultrastruct Res* 32:69–93.
- Sawyer RH, Knapp LW, O'Guin MV. 1986. Epidermis, dermis and appendages. In: Bereiter-Hahn J, Matoltsy AG, Sylvia-Richards K, editors. *Biology of the integument*, Vol 2. Berlin: Springer-Verlag. p 194–237.
- Shames RB, Knapp LW, Carver WE, Sawyer RH. 1988. Identification, expression, and localization of  $\beta$ -keratin gene products during development of avian scutate scales. *Differentiation* 38:115–123.
- Shames RB, Knapp LW, Carver WE, Washington LD, Sawyer RH. 1989. Keratinization of the outer surface of the avian scutate scale: interrelationships of  $\alpha$  and  $\beta$  filaments in a cornifying tissue. *Cell Tiss Res* 257:85–92.
- Shames RB, Knapp LW, Carver WE, Sawyer RH. 1991. Region-specific expression of scutate scale type beta keratins in the developing chick beak. *J Exp Zool* 260:258–266.
- Sun TT, Eichner R, Nelson WG, Tseng SCG, Weiss RA, Jarvinen M, Woodcock-Mitchell J. 1983. Keratin classes: molecular markers for different types of epithelial differentiation. *J Inv Dermatol* 81:109–115.
- Scala C, Cenacchi G, Ferrari C, Pasquinelli G, Preda P, Manara G. 1992. A new acrylic resin formulation: a useful tool for histological, ultrastructural, and immunocytochemical investigations. *J Histochem Cytochem* 40:1799–1804.
- Towbin H, Staehelin T, Gordon J. 1979. Electrophoretic transfer of proteins from polyacrylamide gels to nitrocellulose sheets: procedure and some applications. *Proc Natl Acad Sci USA* 76:4350–4354.
- Woodcock-Mitchell J, Eichner R, Nelson WG, Sun TT. 1982. Immunolocalization of keratin polypeptides in human epidermis using monoclonal antibodies. *J Cell Biol* 95:580–588.
- Wyld JA, Brush AH. 1979. The molecular heterogeneity and diversity of reptilian keratins. *J Mol Evol* 12:331–347.
- Wyld JA, Brush AH. 1983. Keratin diversity in the reptilian epidermis. *J Exp Zool* 225:387–396.